Applied Physics Letters

Tuning of nonlinear vibration via topology variation and its application in energy harvesting

Cite as: Appl. Phys. Lett. **100**, 031902 (2012); https://doi.org/10.1063/1.3676661
Submitted: 27 August 2011 . Accepted: 21 December 2011 . Published Online: 17 January 2012

Xuhan Dai, Xiaodan Miao, Linghe Sui, Hailin Zhou, Xiaolin Zhao, and Guifu Ding

AIP Publishing

Tuning of nonlinear vibration via topology variation and its application in energy harvesting

Xuhan Dai,[a] Xiaodan Miao, Linghe Sui, Hailin Zhou, Xiaolin Zhao, and Guifu Ding
National Key Laboratory of Science and Technology on Nano/Micro Fabrication Technology, Research Institute of Micro/Nano Science and Technology, Shanghai Jiao Tong University, Shanghai 200240, China

(Received 27 August 2011; accepted 21 December 2011; published online 17 January 2012)

A topology variation method for the tuning of nonlinear vibration of planar spring was proposed and experimentally validated, which exhibited great potential for the application of energy harvesting by broadening the response bandwidth of the device. According to the numerical simulation and experimental results of all the three typical topological configurations, the topological scheme with inclined straight shape could provide the best nonlinearity. When this method was applied to the energy harvesting, the prototype device demonstrated a bandwidth of 28 Hz @180 Hz. It is concluded that the topological variation methodology could be efficient for the performance optimization of the energy harvester. © *2012 American Institute of Physics*. [doi:10.1063/1.3676661]

The micro-machined energy harvester is still far away from the commercialization. One of the main obstacles is the stringent requirement of the resonance operation. To maximize the energy transfer efficiency, the frequency of the input vibration should be close to the resonant frequency of the device. This requirement is hard to be met in the real applications. The nonlinear effect was adopted to solve this problem.[1] For example, different types of the snap-through configurations have been reported.[2–7] At the same time, the nonlinear spring was used to broaden the working bandwidth.[8–10] For these nonlinear spring schemes, it was proposed that the bandwidth could be tuned by varying the degree of nonlinearity.[11] The nonlinearity could be set by built-in stress in the structure.[8] However, this method is only suitable for the applications where high excitation levels (up to 25 g in certain cases) exist. Recently, stretching strain was discovered to be effective on inducing significant nonlinearity for ultra-wide bandwidth energy harvesting.[12] The operation frequency of stretching strain scheme was over 1000 Hz, which is much higher than those of many existing ambient vibrations. Therefore, it is necessary to develop efficient methods for tuning the stretch strain effect intentionally. In energy harvester design, this adjustment is critical to meet many specific requirements of the bandwidth and the central frequency in different applications. In this letter, we demonstrated that topological variation could be utilized for the intentional adjustment of stretching strain as mentioned above. At the same time, it could be implemented easily with the batch fabrication process.

Figures 1(a) and 1(b) indicates a typical configuration of the MEMS electromagnetic energy harvester. When the ambient vibration happens, the permanent magnet moves up and down. As a result, the magnetic flux inside the coil varies. Because of electromagnetic induction, there will be electrical potential generated inside the coil. The key component is the spring cantilever, which determines the amplitude and frequency of the magnet vibration. In order to illustrate the influence of topological variation on the characteristics of the cantilever, three topology configurations were investigated. In Fig. 1(b), the cantilever of spring A is the inclined straight bar. For spring B, the cantilever is with one bend. For spring C, there are two bends in the cantilever. The cantilever parameters are shown in Table I. The center platform of the spring is clamped at four corners by the cantilevers. As indicated in Fig. 1(c), when the central platform moves up and down with a large deflection, the distance between the corner and the support increases. This increment will induce the stretching force inside the cantilever. The extent of stretch is dependent on the shape of the cantilever. For spring B and C, the bending feature may compensate for part of the distance increment. In comparison, for spring A, the straight shape bar could not compensate the distance increment as much as B and C. Therefore, the stretch strain in spring A is the heaviest among the three springs. Since the stretching strain could induce significant nonlinear stiffness,[12] the deformation nonlinearity of spring A is larger than that of B and C. Therefore, by variation of the spring topology, the ratio of bending strain and stretching strain at large deformation could be adjusted. In this way, the nonlinear stiffness of the spring could be tuned intentionally by careful consideration of the spring topology.

Finite element analysis was performed in order to validate the effect of topology variation on nonlinear stiffness quantitatively. The stiffness of these springs was analyzed with ANSYS software. The large displacement static analysis was adopted for the solution. The result are shown in Fig. 2(a). The stiffness of the three structures is almost equal in the linear region, where load is less than 2 mN. However, when the deformation of the spring went beyond 100 μm, which is much larger than the thickness of these springs, different nonlinearities come into being. When the load is 10 mN, the static nonlinearity of spring A is over 40% larger than that of B, C. For experimental verification, the springs with the three topology configurations were fabricated with the non-silicon surface micromachining technology.[13] Then their load-deflection characteristics were measured with the

[a]Electronic mail: xhdai@sjtu.edu.cn.

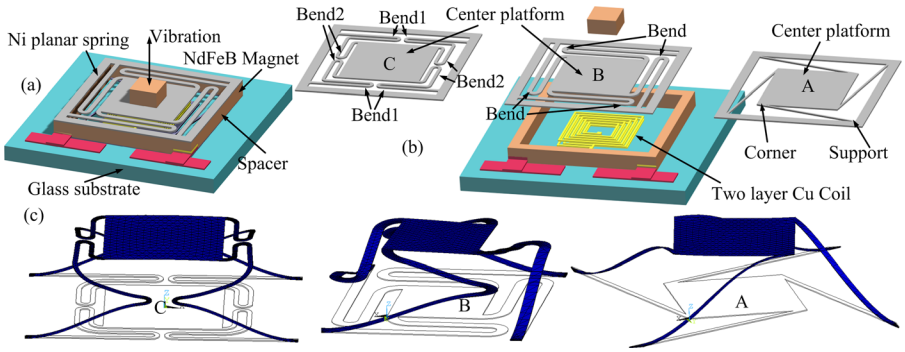

FIG. 1. (Color online) Schematic diagram of the proposed nonlinear tuning methods. (a) configuration of the vibration energy harvester; (b) different topology configurations of the planar springs; (c) deformation of the spring at the large deflection state, the structure in deep color (blue) is the deformed shape, while the black and white figure at the bottom corresponds to the original shape.

TABLE I. Structural parameters of the springs.

Parameters	A	B	C
Spring outer sidelength (mm)		5.7	
Central platform sidelength (mm)		2.5	
Width of beam (μm)	160	300	100
Thickness (μm)	20	25	25

bonding tester (RHESCA, PRT-1101). The tendency and relative ratio of nonlinearity among the springs were verified by the experimental result (Fig. 2(b)). The difference of the absolute deformation value may be induced by the cantilever width and thickness tolerance existed during the fabrication process.

Furthermore, in order to illustrate the influence of the topology variation on the nonlinear vibration, the springs were fixed on a vibrator to observe their response to input vibrations with frequency from 50 to 250 Hz with constant input vibration amplitude of 0.8 g. The moving magnet mass was also kept the same. The amplitude of the spring was measured by the laser displacement sensors (Keyence LK-G30, LK-GD500) and transmitted to the computer to perform the FFT (fast Fourier transformation). In this way, the frequency response (Fig. 3) was obtained. Significant nonlinear resonance was observed for all the three springs. The frequency range between the start and drop point of the nonlinear vibration is defined as the resonance range of the spring. The range of spring A (35 Hz) is almost 60% larger than B (22 Hz) and 75% larger than C (20 Hz), and the central frequency of spring A is over 20 Hz larger than spring C. What is the reason of these different resonant responses?

In this case, the load-deflection characteristic of the spring-mass system can be modeled by the Duffing's equation

$$m \cdot \ddot{z}(t) + d \cdot \dot{z}(t) + k \cdot z(t) + k_n \cdot [z(t)]^3 = -m \cdot \ddot{y}(t)$$

where the symbols are the spring deformation $z(t)$, the mass of moving magnet m, the linear spring stiffness k, the damping ratio d, and the input displacement to the device $y(t)$, k_n is the coefficient determined by the nonlinearity of the deformation. As mentioned above, for the spring A, B, C, the moving magnet mass m are the same ($m_A = m_B = m_C$). According to the feature size of the springs, the damping ratio of spring A and C are less than B ($d_B > d_A$, $d_B > d_C$). The linear stiffness of spring A, B, C are the same ($k_A = k_B = k_C$), while the nonlinear coefficient of spring B and C are less than A ($k_{nA} > k_{nB}$, $k_{nA} > k_{nC}$), as indicated in Fig. 2.

According to the analysis mentioned above, both the air damping effect and nonlinear stiffness may contribute to the difference in the resonant characteristics. For nonlinear vibration, the increment of air damping effect will increase the resonance range.[11] The larger nonlinear coefficient will lead to a wider resonance range and a higher resonance drop point.[11] In Fig. 3, the resonance range of A is larger than B despite the larger air damping ratio d_B than d_A. Therefore, the different resonant response cannot result primarily from the air damping effect. At the same time, as shown in Fig. 3, the resonance range and drop point of spring A is larger than that of B and C. This result confirms the influence of the nonlinear stiffness on resonance range and drop point. In this way, the different nonlinear stiffness induced by the topology variation is concluded to be the main cause of the different

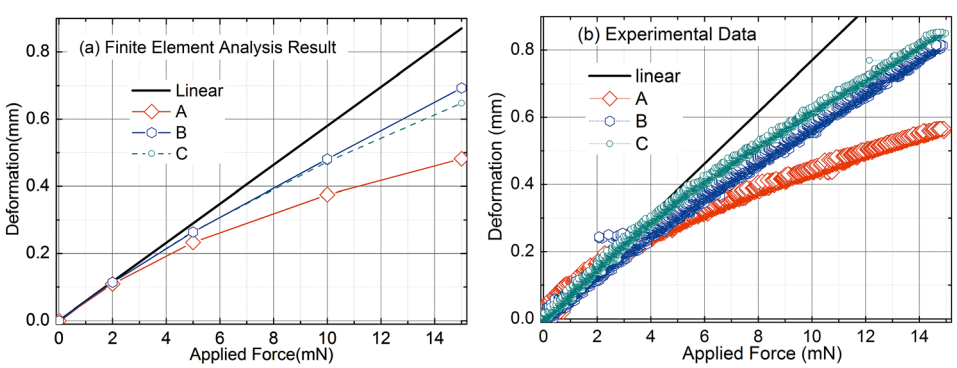

FIG. 2. (Color online) The load–displacement nonlinearity of the three springs with different topology configurations. (a) The calculation result obtained from finite element analysis, (b) the experimental data measured with bonding tester.

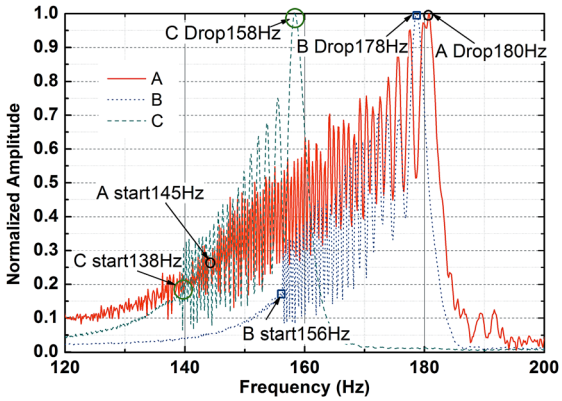

FIG. 3. (Color online) Nonlinear frequency response of the three springs with different topology pattern. The start and drop points for the nonlinear frequency peak climbing process is marked.

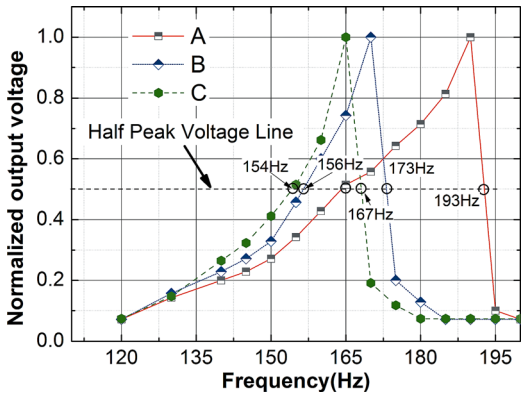

FIG. 5. (Color online) The measured output voltage for harvesters composed of the three different springs. The intersection point between the half peak voltage line and the voltage curve indicates the frequency bandwidth of the device.

resonant characteristics. That is to say, even for spring-mass systems with the same mass and linear stiffness, different resonant characteristics may unveil itself during the nonlinear vibration because of the topology variation. This phenomenon could be utilized in the energy harvester design. By adopting different spring topologies, the central frequency and bandwidth of the harvester may be tuned intentionally to match specific requirements of different applications. However, the deflection amplitude at the start region of the resonance may not be large enough for the generation of the extractable output voltage. Therefore, the actual harvester bandwidth may be not as wide as that of the resonance range. In order to clarify this problem, springs with the three topologies were placed in the prototype electromagnetic energy harvester to measure the output voltage (Fig. 4), respectively. In this way, the influence of the spring topologies on the device actual performance could be declared.

The prototype harvester was fixed on the vibrator and connected with a load resistant (1 MΩ) in series. The internal resistance of the coil is 41Ω. During the increasing frequency sweep from 50 to 250 Hz, the output peak-peak voltage was

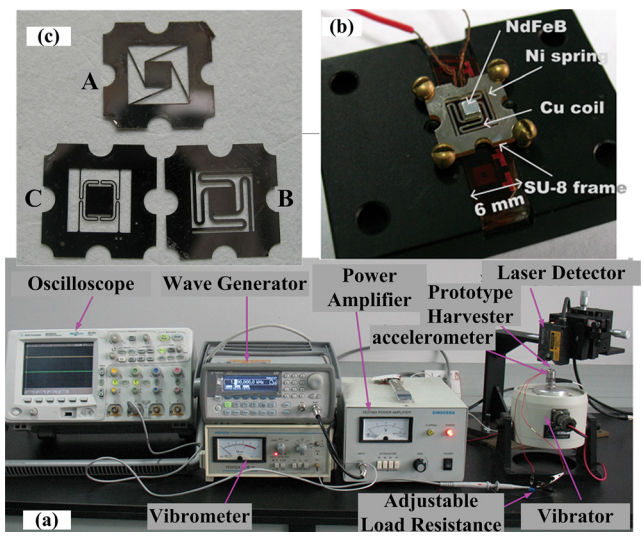

FIG. 4. (Color online) Experimental setup for the frequency response. (a) The equipments used for the measurement, (b) the enlarged view of the prototype harvester, (c) the samples of the three springs with different topology configuration.

measured with the oscilloscope (Agilent, MSO6034A, Fig. 5). If the half peak voltage point is adopted as the criteria of the working bandwidth, the response range of devices and their corresponding percentage of central frequency are 28 Hz/14.7%(A), 17 Hz/10%(B), and 13 Hz/7.8%(C). The maximum output voltage is between 68 and 70 mV. Compared the spectrum of the deflection amplitude with that of the output voltage response, the difference on the central frequency is less than 6%, while the working bandwidth of the voltage response were 20%–35% less than the amplitude resonance range. As suggested above, these differences may be induced by the small deflection amplitude at the start region of the resonance. The amplitude may not be large enough to create significant induced electromotive force. However, the influence of the topology variation on the working bandwidth of the energy harvester is amplified. The working bandwidth of prototype A is over 64% larger than B and more than twice that of C. Therefore, topological variation is proved to be an effective method to broaden the bandwidth of the actual energy harvester. Recently, the cantilever arrays[14] and the mechanical stopper[15] schemes are among the most referenced schemes for wide-band electromagnetic energy harvesters. Compared with these two schemes, shown in Table II, the device volume corresponding to this method is over 1 order of magnitude smaller, while the working bandwidth is in the same order. At the same time, the operation frequency of this method is less than 200 Hz. Since the spring topology is determined by the pattern for optical

TABLE II. Comparison of the performance of different wideband electromagnetic energy harvester schemes (a: acceleration, HVB: half voltage bandwidth, Normalized HVB: percentage of half voltage bandwidth to the central frequency).

Schemes	f_{center} (Hz)	V_{max} (mv)	a (g)	HVB (Hz)	Normalized HVB (%)	Volume (mm^3)	Reference
Ibrahim Sari	4500	10	50	1200	26	$14 \times 12.5 \times 8$	14
M. S. M. Soliman	98	75	0.5	10.5	10.7	$65.3 \times 10 \times 14.3$	15
Topology variation	190	70	0.8	28	14.7	$6 \times 6 \times 3$	——

lithography, this method could be implemented during the mask design stage. The spring characteristic could be varied easily by different pattern design. This is ideal for batch fabrication process. Therefore, this topology variation method provides great opportunities for energy harvesters that have low operation frequency, wide working bandwidth and tiny volumes, which are necessary for applications like wireless sensor networks, embedded biomedical sensors, etc.

The support of the National Science Foundation of China (50977056) is gratefully acknowledged.

[1]D. Zhu, M. J. Tudor, and S. P. Beeby, Meas. Sci. Technol. **21**, 022001 (2010).
[2]F. Cottone, H. Vocca, and L. Gammaitoni, Phys. Rev. Lett. **102**, 080601 (2009).
[3]D. A. W. Barton, S. G. Burrow, and L. R. Clare, Trans. ASME., J. Vib. Acoust. **132**, 021009 (2010).
[4]M. Ferrari, V. Ferrari, M. Guizzetti, B. Ando, S. Baglio, and C. Trigona, Sens. Actuator, A **162**, 425 (2010).
[5]J. T. Lin and B. J. Alphenaar, Intell. Mater. Syst. Struct. **21**, 1337 (2010).
[6]C. R. McInnes, D. G. Gorman, and M. P. Cartmell, J. Sound Vib. **318**, 655 (2008).
[7]S. C. Stanton, C. C. McGehee, and B. P. Mann, Appl. Phys. Lett. **95**, 174103 (2009).
[8]D. Miki, M. Honzumi, Y. Suzuki, and N. Kasagi, in *Proceedings of IEEE MEMS*, Hong Kong, 24–28 January 2010, pp. 176–179.
[9]M. Marzencki, M. Defosseux, and S. Basrour, J. Microelectromech. Syst. **18**, 1444 (2009).
[10]D. S. Nguyen, E. Halvorsen, G. U. Jensen, and A. Vogl, J. Micromech. Microeng. **20**, 125009 (2010).
[11]R. Ramlan, J. Brennan, B. R. Mace, and I. Kovacic, Nonlinear Dyn. **59**, 545 (2010).
[12]A. Hajati and S. Kim, Appl. Phys. Lett. **99**, 083105 (2011).
[13]X. Miao, X. Dai, P. Wang, G. Dinga, and X. Zhao, Microelectron. J. **42**, 992 (2011).
[14]I. Sari, T. Balkan, and H. Kulah, Sens. Actuators A **145–146**, 405 (2008).
[15]M. M. Soliman, E. M. Abdel-Rahman, E. F. El-Saadany, and R. R. Mansour, J. Microelectromech. Syst. **18**, 1288 (2009).